

A parallel-in-time multigrid solver with a new two-level convergence for two-dimensional unsteady fractional Laplacian problems

Xiaoqiang Yue^a, Kejia Pan^{b,*}, Jie Zhou^a, Zhifeng Weng^c, Juan Tang^a, Shi Shu^{a,**}

^a*School of Mathematics and Computational Science, Hunan Key Laboratory for Computation and Simulation in Science and Engineering, Xiangtan University, Hunan 411105, China*

^b*School of Mathematics and Statistics, Central South University, Changsha 410083, China*

^c*School of Mathematical Sciences, Fujian Province University Key Laboratory of Computation Science, Huaqiao University, Fujian 362021, China*

Abstract

The multigrid-reduction-in-time (MGRIT) technique has proven to be successful in achieving higher run-time speedup by exploiting parallelism in time. The goal of this article is to develop and analyze an MGRIT algorithm, using FCF-relaxation with time-dependent time-grid propagators, to seek the finite element approximations of two-dimensional unsteady fractional Laplacian problems. Motivated by [B. S. Southworth, SIAM J. Matrix Anal. Appl. 40 (2019), pp. 564-608], we provide a new temporal eigenvalue approximation property and then deduce a generalized two-level convergence theory which removes the previous unitary diagonalization assumption on the fine and coarse time-grid propagators. Numerical computations are included to confirm theoretical predictions and demonstrate the sharpness of the derived convergence upper bound.

Keywords: fractional Laplacian, Caffarelli-Silvestre extension, reduction-based multigrid, multigrid-in-time, finite element, anisotropic mesh.

1. Introduction

Time-dependent problems involving fractional Laplacian operator are of particular interest in fractional calculus [1–4]. The fractional Laplacian, which is the infinitesimal generator of a standard isotropic α -stable Lévy flight [5], has been used in a broad range of applications including quantum mechanics [6], finance [7], elasticity [8], porous medium [9] and stochastic dynamics [10]. Further details on this topic and equivalent characterizations can be found in the review article [11]. We are concerned in this paper with a non-intrusive parallel time integration with multigrid to a class of two-dimensional unsteady fractional Laplacian problems of the form

$$\begin{cases} \partial_t u(x, y, t) = -(-\Delta)^{\alpha/2} u(x, y, t) + f(x, y, t), & t \in I := (0, T], (x, y) \in \Omega, \\ u(x, y, t) = 0, & t \in I, (x, y) \in \partial\Omega, \\ u(x, y, 0) = \psi_0(x, y), & (x, y) \in \Omega, \end{cases} \quad (1.1)$$

where $\Delta = \partial^2/\partial x^2 + \partial^2/\partial y^2$, the fractional order $\alpha \in (0, 2)$, solution domain $\Omega \subset \mathbb{R}^2$ is an open and bounded subset with Lipschitz continuous boundary $\partial\Omega$.

One of the main challenges of problem (1.1) lies in the nonlocality of the fractional Laplacian. Numerous numerical approximations have been proposed to treat the fractional Laplacian on bounded domains in recent years, such as finite difference [12–21], finite element (FE) [22–29], finite volume [30–32], discontinuous Galerkin [33–36] and

*Xiaoqiang Yue and Kejia Pan contributed equally to this work and should be considered co-first authors.

**Corresponding author.

Email addresses: yuexq@xtu.edu.cn (Xiaoqiang Yue), kejiapan@csu.edu.cn (Kejia Pan), zhouj@xtu.edu.cn (Jie Zhou), zfwmath@163.com (Zhifeng Weng), 1871961655@qq.com (Juan Tang), shushi@xtu.edu.cn (Shi Shu)

spectral (element) [37–46] methods. Utilizing a similar technique to the fractional Laplacian in [47], we can obtain the Caffarelli-Silvestre extension, which is reformulated the original problem posed over Ω on the semi-infinite cylinder $C = \Omega \times (0, +\infty)$ with dynamic boundary condition:

$$\begin{cases} \operatorname{div}(z^\beta \nabla \mathcal{U}) = 0, & t \in I, (x, y, z) \in C, \\ \mathcal{U}(x, y, 0, 0) = \psi_0(x, y), & (x, y) \in \Omega, \\ \mathcal{U}(x, y, z, t) = 0, & t \in I, (x, y, z) \in \partial_L C, \\ d_\alpha \partial_t \mathcal{U} + \partial_\nu^\beta \mathcal{U} = d_\alpha f, & t \in I, (x, y) \in \Omega, z = 0, \end{cases} \quad (1.2)$$

where the parameter $\beta = 1 - \alpha$, the lateral boundary $\partial_L C = \partial\Omega \times [0, +\infty)$, the positive normalization constant d_α and the conormal exterior $\partial_\nu^\beta \mathcal{U}$ are respectively defined by

$$d_\alpha = \frac{2^\beta \Gamma(1 - \alpha/2)}{\Gamma(\alpha/2)} \quad \text{and} \quad \partial_\nu^\beta \mathcal{U} = - \lim_{z \rightarrow 0^+} z^\beta \partial_z \mathcal{U}.$$

A widely used approach to solve nonlocal problem (1.1) is based on the solution of local problem (1.2), however, incorporating one more dimension in space [24, 27]. Specifically, exploiting the intermediate function $\mathcal{U}(x, y, z, t) : C \times I \rightarrow \mathbb{R}$, we immediately get the desired solution $u(x, y, t) : \Omega \times I \rightarrow \mathbb{R}$ subject to the expression $u(x, y, t) = \mathcal{U}(x, y, 0, t)$ for all $(x, y) \in \Omega$ and $t \in I$. It is worthwhile to point out that the anisotropic spatial mesh must be used to capture the singular behavior of $\mathcal{U}(x, y, z, t)$ as $z \rightarrow 0$ [48], and Nochetto et al. have proved the existence and uniqueness for solutions of problems (1.1) and (1.2) (see [49, Theorem 6]) in a purely theoretical manner.

Moving from two-dimensional problems to three-dimensional problems can be difficult for solvers. Chen et al. developed uniformly convergent multilevel methods to tackle steady fractional Laplacian problems [27], which is an important constructive study in the literature. However, a more severe challenge to be faced with arises from the facts that (i) the higher the spatial resolution signifies a comparative or greater scaling in the temporal direction, (ii) future computing speed must rely on the increased concurrency provided by not faster but more processors. The practical consequence is that solution algorithms limited to spatial parallelism for problems with evolutionary behavior shall entail long overall computation time. Therefore, solution algorithms achieving parallelism in time have been of especially high demand. Although time is sequential in essence, parallel-in-time methods are not new and may be dated back to [50, 51]. A recent review of the literature can be found in [52]. At present, parareal in time [53] and multigrid-reduction-in-time (MGRIT) [54] are two of the most popular choices. Wu and Zhou analyzed convergence properties of the parareal algorithm for space fractional diffusion problems [55, 56] and time fractional equations with local time-integrators [57] in constant time-steps. Note that Gander and Vandewalle interpreted parareal as a two-level multigrid full approximation scheme [58], whereas Falgout et al. identified parareal with an optimal two-level MGRIT algorithm and further pointed out that the obvious generalization of parareal to multiple levels couldn't produce an optimal algorithm [54]. In addition, the concurrency of parareal is still limited as its relatively large sequential coarse-grid solve. Conversely, MGRIT, a truly multilevel algorithm implemented in the open-source package XBraid [59], has been proven to be rather effective and analyzed in two-level [60] and multilevel [61] settings, for integer order basic parabolic and hyperbolic problems using L-stable Runge-Kutta schemes, with the limitation on analysis that they only consider the same fine time-grid propagators. Extensions on the two-level convergence analysis to the case of nonuniform temporal meshes are provided in [62, 63]. However, we should point out that only MGRIT using F-relaxation was abstractly discussed in [62] and the unitary diagonalization assumption must be enforced in [63]. Moreover, from the survey of references, there are no calculations taking into account of MGRIT to the fully implicit FE discretization of problem (1.1).

The arrangement of this work proceeds as follows. Section 2 introduces the functional framework and outlines the fully implicit discrete FE scheme. In Section 3, we present the MGRIT V(1,0)-cycle algorithm using FCF-relaxation followed by a generalized two-level convergence analysis without the assumption of unitary diagonalization. Section 4 conducts numerical experiments to illustrate the optimal order of convergence and the computational error-norms decay rate of the fully discrete FE scheme, the robustness of Chen's multigrid with line smoother with respect to the fractional order α and the spatial mesh size, as well as the sharpness of the derived convergence upper bound on the two-level MGRIT algorithm. Finally, in Section 5, we draw some conclusions and discuss future work.

2. Mathematical preliminaries

This section is devoted to introducing some mathematical preliminaries, including the variational formulation of the local problem (1.2) and its fully implicit discrete FE scheme.

2.1. The variational formulation

Let $\mathcal{D} \subset \mathbb{R}^3$ be open, $L^2(\mathcal{z}^\beta, \mathcal{D})$ and $H^1(\mathcal{z}^\beta, \mathcal{D})$ denote the weighted Lebesgue and Sobolev spaces [64]

$$L^2(\mathcal{z}^\beta, \mathcal{D}) = \{w : \int_{\mathcal{D}} \mathcal{z}^\beta w^2 < +\infty\}, \quad H^1(\mathcal{z}^\beta, \mathcal{D}) = \{v \in L^2(\mathcal{z}^\beta, \mathcal{D}) : |\nabla v| \in L^2(\mathcal{z}^\beta, \mathcal{D})\},$$

with norms

$$\|w\|_{L^2(\mathcal{z}^\beta, \mathcal{D})} = \left(\int_{\mathcal{D}} \mathcal{z}^\beta w^2 \right)^{\frac{1}{2}}, \quad \|v\|_{H^1(\mathcal{z}^\beta, \mathcal{D})} = \left(\|v\|_{L^2(\mathcal{z}^\beta, \mathcal{D})}^2 + \|\nabla v\|_{L^2(\mathcal{z}^\beta, \mathcal{D})}^2 \right)^{\frac{1}{2}},$$

where ∇v is the distributional gradient of the measurable function v .

Since $\beta \in (-1, 1)$, weight \mathcal{z}^β belongs to the Muckenhoupt class $A_2(\mathbb{R}^3)$ [65], which implies that $H^1(\mathcal{z}^\beta, \mathcal{D})$ is Hilbert. In order to settle problem (1.2), we define

$$\mathring{H}_L^1(\mathcal{z}^\beta, \mathcal{D}) := \{v \in H^1(\mathcal{z}^\beta, \mathcal{D}) : v = 0 \text{ on } \partial_L \mathcal{D}\}, \quad \mathbb{H}^{\alpha/2}(\Omega) = [H_0^1(\Omega), L^2(\Omega)]_{1-\alpha/2} \text{ and } \mathbb{H}^{-\alpha/2}(\Omega) \text{ as the dual of } \mathbb{H}^{\alpha/2}(\Omega).$$

Thus, given a forcing term $f \in L^2(0, T; \mathbb{H}^{-\alpha/2}(\Omega))$ and an initial datum $\psi_0 \in L^2(\Omega)$, the function $u \in \mathbb{W}$ solves problem (1.1) if and only if its harmonic extension $\mathcal{U} \in \mathbb{V}$ solves problem (1.2), where

$$\mathbb{W} := \{w \in L^\infty(0, T; L^2(\Omega)) \cap L^2(0, T; \mathbb{H}^{\alpha/2}(\Omega)) : \partial_t w \in L^2(0, T; \mathbb{H}^{-\alpha/2}(\Omega))\}$$

and

$$\mathbb{V} := \{v \in L^2(0, T; \mathring{H}_L^1(\mathcal{z}^\beta, C)) : \partial_t \text{tr}_\Omega v \in L^2(0, T; \mathbb{H}^{-\alpha/2}(\Omega))\}.$$

Recall that the trace operator tr_Ω onto $\Omega \times \{z = 0\}$ satisfies (see [24, Proposition 2.5])

$$\mathring{H}_L^1(\mathcal{z}^\beta, C) \ni w \mapsto \text{tr}_\Omega w \in \mathbb{H}^{\alpha/2}(\Omega),$$

we get the variational formulation of problem (1.2): to find $\tilde{\mathcal{U}} \in \mathbb{V}$ subject to $\text{tr}_\Omega \tilde{\mathcal{U}}|_{t=0} = \psi_0$ and

$$\langle \text{tr}_\Omega \partial_t \tilde{\mathcal{U}}, \text{tr}_\Omega \phi \rangle_\alpha + \frac{1}{d_\alpha} \int_C (\mathcal{z}^\beta \nabla \tilde{\mathcal{U}}) \cdot \nabla \phi = \langle f, \text{tr}_\Omega \phi \rangle_\alpha, \quad \forall \phi \in \mathring{H}_L^1(\mathcal{z}^\beta, C), \quad \text{a.e. } t \in I, \quad (2.1)$$

where $\langle \cdot, \cdot \rangle_\alpha$ is the duality pairing between $\mathbb{H}^{-\alpha/2}(\Omega)$ and $\mathbb{H}^{\alpha/2}(\Omega)$.

2.2. The fully implicit discrete FE scheme

Note that problem (1.2) can't be approximated except that C is truncated to $C_{\mathcal{Z}} := \Omega \times (0, \mathcal{Z})$ for a suitable $\mathcal{Z} < +\infty$ with $\partial_L C_{\mathcal{Z}} = \partial\Omega \times [0, \mathcal{Z}) \cup \Omega \times \{z = \mathcal{Z}\}$ and an additional homogeneous Dirichlet on $z = \mathcal{Z}$, whose theoretical foundation is the exponential decay of $\tilde{\mathcal{U}}$ in the extended direction z on the basis of the length \mathcal{Z} , see [49, Proposition 22].

The first step toward the discretization is to obtain a semi-discrete approximation of the truncated problem of the original problem (2.1). To do so, we associate a (possibly nonuniform) mesh by points $0 = t_0 < t_1 < \dots < t_N = T$ and time step sizes $\tau_j = t_j - t_{j-1}$ for $j = 1, \dots, N$. The backward Euler discretization is applied: to seek $\{U_k\}_{k=0}^N \subset \mathring{H}_L^1(\mathcal{z}^\beta, C_{\mathcal{Z}})$ subject to $\text{tr}_\Omega U_0 = \psi_0$ and

$$\left(\frac{\text{tr}_\Omega U_{k+1} - \text{tr}_\Omega U_k}{\tau_{k+1}}, \text{tr}_\Omega \vartheta \right)_{L^2(\Omega)} + \frac{1}{d_\alpha} \int_{C_{\mathcal{Z}}} (\mathcal{z}^\beta \nabla U_{k+1}) \cdot \nabla \vartheta = \langle f_{k+1}, \text{tr}_\Omega \vartheta \rangle_\alpha, \quad k = 0, \dots, N-1$$

for all $\vartheta \in \dot{H}_L^1(z^\beta, C_Z)$, where $f_{k+1} := f|_{I_{k+1}}$. Obviously, the sequence

$$\{u_k := \text{tr}_\Omega U_k \in \mathbb{H}^{\alpha/2}(\Omega)\}_{k=1}^N$$

is a series of piecewise constant approximations to the solution of problem (1.1).

Next, we turn to discuss the spatial discretization. Given a quasi-uniform triangulation \mathcal{T}_Ω over Ω and a graded partition \mathcal{J}_Z of $[0, Z]$ by the transition points

$$z_j = \begin{cases} z_* \mathcal{Z} \left(\frac{4j}{3M} \right)^\mu, & 0 \leq j \leq \frac{3}{4}M \\ \mathcal{Z} \left[(1 - z_*) \left(\frac{4j}{M} - 3 \right) + z_* \right], & \frac{3}{4}M < j \leq M \end{cases} \quad \text{with } \mu = \frac{3}{\alpha} + 0.01, \quad z_* = \left(1 + \frac{\mu}{3} \right)^{-1} \quad (2.2)$$

as well as segments $I_k = (z_{k-1}, z_k)$ for $k = 1, \dots, M$, we construct the mesh \mathcal{J} over C_Z as the tensor product of \mathcal{T}_Ω and \mathcal{J}_Z , and define

$$\mathbb{V}(\mathcal{J}) := \{v \in C(\bar{C}_Z) : v|_{K \times I_k} \in \mathcal{P}_1(K) \otimes \mathcal{P}_1(I_k), \forall K \in \mathcal{T}_\Omega, 1 \leq k \leq M; v|_{\partial_L C_Z} = 0\}, \quad \mathbb{W}(\mathcal{J}_\Omega) := \text{tr}_\Omega \mathbb{V}(\mathcal{J}),$$

and the weighted elliptic projector $\mathcal{L} : \dot{H}_L^1(z^\beta, C_Z) \rightarrow \mathbb{V}(\mathcal{J})$ such that

$$\int_{C_Z} [z^\beta \nabla(\mathcal{L}w)] \cdot \nabla v = \int_{C_Z} (z^\beta \nabla w) \cdot \nabla v, \quad \forall v \in \mathbb{V}(\mathcal{J})$$

is valid for any function $w \in \dot{H}_L^1(z^\beta, C_Z)$, where \mathcal{P}_1 denotes the space of all polynomials of at most one degree.

Finally, we arrive at the fully discrete FE scheme: with the initial guess $U_0^\mathcal{J} := (\mathcal{L} \circ \text{tr}_\Omega^{-1})\psi_0$, to calculate $\{U_k^\mathcal{J}\}_{k=1}^N \subset \mathbb{V}(\mathcal{J})$ satisfying the constraint

$$\left(\frac{\text{tr}_\Omega U_{k+1}^\mathcal{J} - \text{tr}_\Omega U_k^\mathcal{J}}{\tau_{k+1}}, \text{tr}_\Omega v \right)_{L^2(\Omega)} + \frac{1}{d_\alpha} \int_{C_Z} (z^\beta \nabla U_{k+1}^\mathcal{J}) \cdot \nabla v = \langle f_{k+1}, \text{tr}_\Omega v \rangle_\alpha, \quad \forall v \in \mathbb{V}(\mathcal{J}). \quad (2.3)$$

As before, approximate solutions of problem (1.1) are given by

$$\{u_k^\mathcal{J} := \text{tr}_\Omega U_k^\mathcal{J} \in \mathbb{W}(\mathcal{J})\}_{k=1}^N.$$

In order to get the matrix formulation of (2.3), it is necessary to introduce

$$\mathbb{U}(\mathcal{J}_\Omega) = \{u_h \in H_0^1(\Omega) : u_h \in C(\Omega), u_h|_K \in \mathcal{P}_1(K), \forall K \in \mathcal{T}_\Omega\} = \text{span}\{\phi_i, i = 1, \dots, n\}$$

and

$$\mathbb{Z}(\mathcal{J}_Z) = \{z_h \in H_0^1(0, Z) : z_h|_{I_k} \in \mathcal{P}_1(I_k), 1 \leq k \leq M\} = \text{span}\{\psi_j, j = 1, \dots, M-1\},$$

where n is the number of interior vertices in \mathcal{T}_Ω . It is straightforward to verify that $\mathbb{V}(\mathcal{J})$ and $U_k^\mathcal{J}$ can be respectively written as

$$\mathbb{V}(\mathcal{J}) = \text{span}\{\phi_i \psi_j, i = 1, \dots, n; j = 1, \dots, M-1\} \quad \text{and} \quad U_k^\mathcal{J} = \sum_{i=1}^n \sum_{j=1}^{M-1} u_{ij}^{(k)} \phi_i \psi_j.$$

Choosing the test function $v = \phi_q \psi_l$ in (2.3), we deduce

$$\int_{C_Z} [(z^\beta \psi_j \nabla \phi_i) \cdot (\phi_q \nabla \psi_l) + (z^\beta \phi_i \nabla \psi_j) \cdot (\psi_l \nabla \phi_q)] = 0$$

by Green's first identity and the fact that $\phi_i|_{\partial\Omega} = \phi_q|_{\partial\Omega} = 0$, and one further expansion via separation of variables

$$\frac{1}{d_\alpha} \int_{C_Z} [z^\beta \nabla(\phi_i \psi_j)] \cdot \nabla(\phi_q \psi_l) = a_{iq}^s m_{jl}^z + m_{iq}^s a_{jl}^z,$$

where entries

$$a_{iq}^s = \frac{1}{d_\alpha} \int_{\Omega} \nabla \phi_i \nabla \phi_q, \quad m_{jl}^z = \int_0^Z z^\beta \psi_j \psi_l, \quad m_{iq}^s = \frac{1}{d_\alpha} \int_{\Omega} \phi_i \phi_q \quad \text{and} \quad a_{jl}^z = \int_0^Z z^\beta \frac{d\psi_j}{dz} \frac{d\psi_l}{dz}.$$

Thus, the system of linear equations obtained from (2.3) is of the form

$$\left(\frac{1}{\tau_{k+1}} \begin{bmatrix} M_s & O \\ O & O \end{bmatrix} + M_z \otimes A_s + A_z \otimes M_s \right) \begin{bmatrix} \mathcal{U}_{k+1} \\ \mathcal{V}_{k+1} \end{bmatrix} = \frac{1}{\tau_{k+1}} \begin{bmatrix} M_s & O \\ O & O \end{bmatrix} \begin{bmatrix} \mathcal{U}_k \\ \mathcal{V}_k \end{bmatrix} + \begin{bmatrix} \mathcal{F}_{k+1} \\ O \end{bmatrix}, \quad k = 0, \dots, N-1, \quad (2.4)$$

where

- matrixes $M_z = (m_{ij}^z)_{(M-1) \times (M-1)}$, $A_z = (a_{ij}^z)_{(M-1) \times (M-1)}$, $M_s = (m_{ij}^s)_{n \times n}$ and $A_s = (a_{ij}^s)_{n \times n}$,
- O represents a zero matrix of suitable size, \otimes denotes the Kronecker product,
- $\mathcal{U}_k = (u_{11}^{(k)}, \dots, u_{1n}^{(k)})^T$ with $u_{1i}^{(0)} = \tilde{\psi}_0(x_i, y_i)$ for $i = 1, \dots, n$ to approximate the initial $\psi_0(x, y)$,
- $\mathcal{V}_k = (u_{21}^{(k)}, \dots, u_{2n}^{(k)}; \dots; u_{(M-1)1}^{(k)}, \dots, u_{(M-1)n}^{(k)})^T$ is the auxiliary vector produced by the other points in the extended direction,
- $\mathcal{F}_{k+1} = (f_1^{(k+1)}, \dots, f_n^{(k+1)})^T$ with $f_i^{(k+1)} = \langle f_{k+1}, \phi_i \rangle_\alpha$.

It is trivial to see that the coefficient matrix of (2.4) is symmetric positive definite (SPD). Therefore, the multigrid with line smoother proposed in [27] is a very suitable method and is employed in our implementation.

3. MGRIT formulation and a generalized two-level convergence upper bound

The main focus of this section is the general MGRIT algorithm using FCF-relaxation, followed by its two-level convergence analysis for the general case where the time-grid propagators don't have to be the same and need not be simultaneously diagonalizable with a unitary matrix.

3.1. The general MGRIT algorithm using FCF-relaxation

Consider the following block unit lower bidiagonal system

$$\mathcal{AU} := \begin{bmatrix} I & & & \\ -\Psi_1 & I & & \\ & \ddots & \ddots & \\ & & -\Psi_N & I \end{bmatrix} \begin{bmatrix} \mathcal{U}_0 \\ \mathcal{U}_1 \\ \vdots \\ \mathcal{U}_N \end{bmatrix} = \begin{bmatrix} \mathcal{G}_0 \\ \mathcal{G}_1 \\ \vdots \\ \mathcal{G}_N \end{bmatrix} := \mathcal{G}, \quad (3.1)$$

where $\mathcal{G}_0 = \mathcal{U}_0$, I is the identity matrix, vectors $\{\mathcal{U}_j\}_{j=1}^N$, $\{\mathcal{G}_j\}_{j=1}^N$ and time-grid propagators $\{\Psi_j\}_{j=1}^N$ are assumed not to be connected with any specific forms.



Figure 1: Schematic view of the CF-splitting by a factor of four.

Various components are required in order to solve the global space-time problem (3.1) through the MGRIT algorithm based on the multigrid reduction technique [66]. Define the coarse temporal mesh with nodes $\{\tilde{t}_i := t_{m \times i}\}_{i=0}^{N_c}$ and time step sizes $\{\tilde{\tau}_j = \tilde{t}_j - \tilde{t}_{j-1}\}_{j=1}^{N_c}$ for some coarsening factor m , where $N_c = N/m$. Then all \tilde{t}_i are disconnected C-points representing those variables in the coarse level and the others are F-points grouped $m-1$ adjacent points into a bunch. The particular case when $m = 4$ is illustrated in Fig. 1. It should be mentioned that $\{\tilde{t}_i\}_{i=0}^{N_c}$ is still viewed to be nonuniform. Assume for simplicity of presentation here that F-points are ordered first. MGRIT utilizes the coarse injection $[0, I_c]$ as the restriction operator, i.e., only the residual at C-points is computed, where I_c is the identity matrix.

The FCF-relaxation (i.e., an initial F-relaxation followed by a C-relaxation and then a second F-relaxation) is often the most preferable choice to produce optimal and scalable multilevel iterations [54], where F-relaxation refers to updating variables at $m - 1$ F-points in turn yet independent of other F-intervals, and C-relaxation stands for performing (2.4) to propagate the solution at a C-point. It is apparent that these two processes are both highly parallel. The ideal interpolation is used to provide the coarse-grid correction, which is implemented at the cost of updating C-variables by the coarse approximations immediately followed by an F-relaxation over the time-grid propagators $\{\Psi_j\}_{j=1}^N$. It is worth mentioning that the resulting Petrov-Galerkin triple matrix product is exactly the Schur complement

$$\mathcal{A}_\Delta = \begin{bmatrix} I & & & & \\ -\mathcal{B}_{\Psi,m}^m & I & & & \\ & -\mathcal{B}_{\Psi,2m}^m & I & & \\ & & \ddots & \ddots & \\ & & & -\mathcal{B}_{\Psi,N}^m & I \end{bmatrix}, \quad (3.2)$$

where $\mathcal{B}_{\Psi,s}^l = \Psi_s \Psi_{s-1} \cdots \Psi_{s-l+1}$ with $\mathcal{B}_{\Psi,s}^0 = I$, positive integer s and nonnegative integer l . However, this coarse-grid problem would be as expensive as the original fine-grid problem. MGRIT approximates the coarse-grid operator with

$$\mathcal{S}_\Delta = \begin{bmatrix} I & & & & \\ -\Phi_1 & I & & & \\ & -\Phi_2 & I & & \\ & & \ddots & \ddots & \\ & & & -\Phi_{N_c} & I \end{bmatrix}, \quad (3.3)$$

where Φ_k ($k = 1, \dots, N_c$) is an approximate coarse-grid time-stepping operator to $\mathcal{B}_{\Psi,km}^m$. The most natural choice of Φ_k is to re-discretize the time-dependent linear continuous problem on the coarse temporal mesh. The final stage is the application of the above processes recursively, with possibly different coarsening factors at different time levels, to construct a multilevel hierarchy under certain stopping criteria, e.g., by setting the maximum number of time levels and the minimum coarsest temporal grid size. Below is a sketch of the resulting MGRIT V(1,0)-cycle algorithm using FCF-relaxation in the recursive fashion, where L is the number of time levels determined by the user supplied stopping procedure, $\mathcal{A}^{(1)} = \mathcal{A}$, $\mathcal{G}^{(1)} = \mathcal{G}$, matrices $\mathcal{A}^{(k+1)}$, $\mathcal{R}^{(k)}$ and $\mathcal{P}^{(k)}$ ($k = 1, \dots, L - 1$) respectively correspond to the k -th coarse-scale time re-discretization, the mentioned above restriction and interpolation.

Algorithm 1. MGRIT V(1,0)-cycle algorithm using FCF-relaxation: $\mathcal{U}^{(k)} = \text{MGRIT}(k, \mathcal{A}^{(k)}, \mathcal{U}^{(k)}, \mathcal{G}^{(k)})$

Step 1 Apply FCF-relaxation to $\mathcal{A}^{(k)}\mathcal{U}^{(k)} = \mathcal{G}^{(k)}$ with $\mathcal{U}^{(k)}$ as the initial guess.

Step 2 Inject the residual to the coarse time level $\mathcal{G}^{(k+1)} = \mathcal{R}^{(k)}(\mathcal{G}^{(k)} - \mathcal{A}^{(k)}\mathcal{U}^{(k)})$.

Step 3 If $k + 1 = L$, then solve $\mathcal{A}^{(L)}\mathcal{U}^{(L)} = \mathcal{G}^{(L)}$; Else compute $\mathcal{U}^{(k+1)} = \text{MGRIT}(k + 1, \mathcal{A}^{(k+1)}, 0, \mathcal{G}^{(k+1)})$.

Step 4 Perform the coarse-grid correction using the ideal interpolation $\mathcal{U}^{(k)} = \mathcal{U}^{(k)} + \mathcal{P}^{(k)}\mathcal{U}^{(k+1)}$.

Remark 1. (Reduction of the computational overhead) Here, we point out that Step 4 of Algorithm 1 is executed by just correcting C-variables, and updating F-variables only when the Euclidean norm of the residual is small enough. The underlying reason is that corrections at F-points are equivalent to an F-relaxation, which will be performed in the subsequent MGRIT iteration.

3.2. A generalized two-level convergence analysis

Setting $L = 2$, Algorithm 1 in this case reduces to the well-known two-level scheme, whose residual propagation operator for a single iteration, as in the derivations of [62, 63], can be expressed as in an FC-partitioning of \mathcal{A} :

$$\mathcal{R}_{TL}^{FCF} = \begin{bmatrix} 0 \\ \mathcal{T}_\Psi^\Phi \end{bmatrix} [Q \ I], \quad \mathcal{T}_\Psi^\Phi = (I - \mathcal{A}_\Delta \mathcal{S}_\Delta^{-1})(I - \mathcal{A}_\Delta), \quad (3.4)$$

where the matrix used in forming the “ideal restriction” operator

$$Q = \begin{bmatrix} 0 & \cdots & 0 & 0 \\ \mathcal{B}_{\Psi,m}^{m-1} & \cdots & \mathcal{B}_{\Psi,m}^2 & \mathcal{B}_{\Psi,m}^1 & & \\ & & \mathcal{B}_{\Psi,2m}^{m-1} & \cdots & \mathcal{B}_{\Psi,2m}^2 & \mathcal{B}_{\Psi,2m}^1 & & \\ & & & & \ddots & & & \\ & & & & & \mathcal{B}_{\Psi,N}^{m-1} & \cdots & \mathcal{B}_{\Psi,N}^2 & \mathcal{B}_{\Psi,N}^1 \end{bmatrix}.$$

Below, we wish to find an upper bound for a certain norm of the residual propagation \mathcal{R}_{TL}^{FCF} .

S1 Assume that time-stepping operators Ψ_j and Φ_k are both strongly stable [67] (i.e., the discrete l^2 -norms $\|\Psi_j\| < 1$ and $\|\Phi_k\| < 1$) and simultaneously diagonalizable by the matrix \mathcal{X}_s . Note that the assumption on simultaneous diagonalization will be tenable when the same spatial discretization is exploited on fine and coarse temporal meshes. Denote by $\{\lambda_j^{(\omega)}\}_{\omega=1}^n$ and $\{\mu_k^{(\omega)}\}_{\omega=1}^n$ the sets of all complex eigenvalues of Ψ_j and Φ_k , respectively.

S2 Through simple algebraic calculations, we arrive at an estimate of the second term in (3.4):

$$\|[Q \ I]\| = \sqrt{\lambda_{\max}\left(\begin{bmatrix} Q^T \\ I \end{bmatrix} [Q \ I]\right)} = \max_k \sqrt{\left\|\sum_{i=0}^{m-1} \mathcal{B}_{\Psi,km}^i (\mathcal{B}_{\Psi,km}^i)^T\right\|} \leq \max_k \sqrt{\sum_{i=0}^{m-1} \|\mathcal{B}_{\Psi,km}^i\|^2}.$$

From the relation $\|\Psi_j\| < 1$ for $j = 1, \dots, N$ in Stage **S1**, we have

$$\|\mathcal{B}_{\Psi,km}^0\| = 1, \quad \|\mathcal{B}_{\Psi,km}^i\| \leq \|\Psi_{km}\| \cdot \|\Psi_{km-1}\| \cdots \|\Psi_{km-i+1}\| < 1 \text{ for } i = 1, \dots, m-1,$$

and hence $\|[Q \ I]\| < \sqrt{m}$.

S3 By exploiting the closed form

$$\mathcal{S}_{\Delta}^{-1} = \begin{bmatrix} I & & & & \\ \mathcal{B}_{\Phi,1}^1 & I & & & \\ \mathcal{B}_{\Phi,2}^2 & \mathcal{B}_{\Phi,2}^1 & I & & \\ \vdots & \vdots & \ddots & \ddots & \\ \mathcal{B}_{\Phi,N_c}^{N_c} & \mathcal{B}_{\Phi,N_c}^{N_c-1} & \cdots & \mathcal{B}_{\Phi,N_c}^1 & I \end{bmatrix},$$

the other two matrix forms appeared in \mathcal{R}_{TL}^{FCF} are obtained from block lower bidiagonal structures (3.2)-(3.3):

$$I - \mathcal{A}_{\Delta} \mathcal{S}_{\Delta}^{-1} = \begin{bmatrix} 0 & & & & \\ \mathcal{B}_{\Psi,m}^m - \Phi_1 & 0 & & & \\ (\mathcal{B}_{\Psi,2m}^m - \Phi_2) \mathcal{B}_{\Phi,1}^1 & \mathcal{B}_{\Psi,2m}^m - \Phi_2 & 0 & & \\ \vdots & \vdots & \ddots & \ddots & \\ (\mathcal{B}_{\Psi,N}^m - \Phi_{N_c}) \mathcal{B}_{\Phi,N_c}^{N_c-1} & (\mathcal{B}_{\Psi,N}^m - \Phi_{N_c}) \mathcal{B}_{\Phi,N_c}^{N_c-2} & \cdots & \mathcal{B}_{\Psi,N}^m - \Phi_{N_c} & 0 \end{bmatrix}$$

and

$$I - \mathcal{A}_{\Delta} = \begin{bmatrix} 0 & & & & \\ \mathcal{B}_{\Psi,m}^m & 0 & & & \\ & \mathcal{B}_{\Psi,2m}^m & 0 & & \\ & & \ddots & \ddots & \\ & & & \mathcal{B}_{\Psi,N}^m & 0 \end{bmatrix}.$$

As a result, the expression of \mathcal{T}_Ψ^Φ can be rewritten as

$$\mathcal{T}_\Psi^\Phi = \begin{bmatrix} 0 & & & & & \\ 0 & & 0 & & & \\ (\mathcal{B}_{\Psi,2m}^m - \Phi_2)\mathcal{B}_{\Psi,m}^m & & 0 & 0 & & \\ (\mathcal{B}_{\Psi,3m}^m - \Phi_3)\mathcal{B}_{\Phi,2}^1\mathcal{B}_{\Psi,m}^m & (\mathcal{B}_{\Psi,3m}^m - \Phi_3)\mathcal{B}_{\Psi,2m}^m & 0 & 0 & & \\ \vdots & \vdots & \ddots & \ddots & \ddots & \\ (\mathcal{B}_{\Psi,N}^m - \Phi_{N_c})\mathcal{B}_{\Phi,N_c-1}^{N_c-2}\mathcal{B}_{\Psi,m}^m & (\mathcal{B}_{\Psi,N}^m - \Phi_{N_c})\mathcal{B}_{\Phi,N_c-1}^{N_c-3}\mathcal{B}_{\Psi,2m}^m & \cdots & (\mathcal{B}_{\Psi,N}^m - \Phi_{N_c})\mathcal{B}_{\Psi,N-m}^m & 0 & 0 \end{bmatrix}, \quad (3.5)$$

which can be reformulated as the under-mentioned triple matrix product

$$\begin{bmatrix} I & & & & \\ & I & & & \\ & & \mathcal{B}_{\Psi,2m}^m - \Phi_2 & & \\ & & & \ddots & \\ & & & & \mathcal{B}_{\Psi,N}^m - \Phi_{N_c} \end{bmatrix} \begin{bmatrix} 0 & & & & \\ 0 & 0 & & & \\ I & 0 & 0 & & \\ \mathcal{B}_{\Phi,2}^1 & I & 0 & 0 & \\ \vdots & \vdots & \ddots & \ddots & \ddots \\ \mathcal{B}_{\Phi,N_c-1}^{N_c-2} & \mathcal{B}_{\Phi,N_c-1}^{N_c-3} & \cdots & I & 0 & 0 \end{bmatrix} \begin{bmatrix} \mathcal{B}_{\Psi,m}^m & & & & \\ & \ddots & & & \\ & & \mathcal{B}_{\Psi,N-m}^m & & \\ & & & I & \\ & & & & I \end{bmatrix}.$$

Then, under the assumption that $\mathcal{B}_{\Psi,jm}^m - \Phi_j$ is invertible for $j = 2, \dots, N_c$, using the relation $\mathcal{B}_{\Phi,s}^k = \mathcal{B}_{\Phi,s}^l \mathcal{B}_{\Phi,s-l}^{k-l}$, and recalling that the Moore-Penrose conditions are used to define the pseudoinverse D^\dagger of any matrix D :

$$DD^\dagger \text{ and } D^\dagger D \text{ are both Hermitian, } DD^\dagger D = D \text{ and } D^\dagger DD^\dagger = D^\dagger,$$

the unique pseudoinverse $(\mathcal{T}_\Psi^\Phi)^\dagger$ of \mathcal{T}_Ψ^Φ can be established in a straightforward way

$$(\mathcal{T}_\Psi^\Phi)^\dagger = \begin{bmatrix} 0 & 0 & t_2^\dagger & & \\ 0 & 0 & g_2^\dagger & t_3^\dagger & \\ & & \ddots & \ddots & \\ & & & g_{N_c-1}^\dagger & t_{N_c}^\dagger \\ & & & 0 & 0 \\ & & & 0 & 0 \end{bmatrix} \quad \text{with} \quad \begin{aligned} t_l^\dagger &= (\mathcal{B}_{\Psi,(l-1)m}^m)^{-1}(\mathcal{B}_{\Psi,lm}^m - \Phi_l)^{-1}, \quad l = 2, \dots, N_c, \\ g_s^\dagger &= -(\mathcal{B}_{\Psi,sm}^m)^{-1}\Phi_s(\mathcal{B}_{\Psi,sm}^m - \Phi_s)^{-1}, \quad s = 2, \dots, N_c - 1, \end{aligned} \quad (3.6)$$

by noticing the following two important results

$$\mathcal{T}_\Psi^\Phi (\mathcal{T}_\Psi^\Phi)^\dagger = \begin{bmatrix} 0 & & & & \\ & 0 & & & \\ & & I & & \\ & & & \ddots & \\ & & & & I \end{bmatrix}, \quad (\mathcal{T}_\Psi^\Phi)^\dagger \mathcal{T}_\Psi^\Phi = \begin{bmatrix} I & & & & \\ & \ddots & & & \\ & & I & & \\ & & & 0 & \\ & & & & 0 \end{bmatrix}.$$

It is easy to see that the use of $(\mathcal{T}_\Psi^\Phi)^\dagger$ allows for a simpler technical path to analyze the maximum singular value of \mathcal{T}_Ψ^Φ through the minimum nonzero singular value of $(\mathcal{T}_\Psi^\Phi)^\dagger$ with the advantage of its simplicity.

S4 Based on the simultaneous diagonalizability from Stage **S1**:

$$\mathcal{X}_s^{-1} \Psi_j \mathcal{X}_s = \mathbf{diag}(\lambda_j^{(1)}, \dots, \lambda_j^{(n)}) := \Lambda_j, \quad j = 1, \dots, N; \quad \mathcal{X}_s^{-1} \Phi_k \mathcal{X}_s = \mathbf{diag}(\mu_k^{(1)}, \dots, \mu_k^{(n)}) := \Upsilon_k, \quad k = 1, \dots, N_c,$$

we have

$$\|\mathcal{T}_\Psi^\Phi\|_{(\tilde{\mathcal{X}}_s, \tilde{\mathcal{X}}_s^*)^{-1}} = \sup_{v \neq 0} \frac{\|\tilde{\mathcal{X}}_s^{-1} \mathcal{T}_\Psi^\Phi \tilde{\mathcal{X}}_s \tilde{\mathcal{X}}_s^{-1} v\|}{\|\tilde{\mathcal{X}}_s^{-1} v\|} = \sup_{w \neq 0} \frac{\|\mathcal{P}_s \mathcal{T}_\Lambda^\Upsilon \mathcal{P}_s^T w\|}{\|w\|} = \max_{\omega} \|[\mathcal{T}_\Lambda^\Upsilon]_{\omega}\| = \frac{1}{\min_{\omega} \sigma_{\min}([\mathcal{T}_\Lambda^\Upsilon]_{\omega})},$$

where

- $\tilde{\mathcal{X}}_s = \mathbf{diag}(\mathcal{X}_s, \dots, \mathcal{X}_s)$ consisting of $N_c + 1$ diagonal blocks,
- $\mathcal{T}_\Lambda^\Upsilon$ and $(\mathcal{T}_\Lambda^\Upsilon)^\dagger$ are obtained from replacing Ψ, Φ by Λ, Υ in (3.5) and (3.6), respectively,
- \mathcal{P}_s denotes the orthogonal permutation matrix which makes $\mathcal{P}_s \mathcal{T}_\Lambda^\Upsilon \mathcal{P}_s^T$ block diagonal,
- $[\mathcal{T}_\Lambda^\Upsilon]_\omega$ and $[(\mathcal{T}_\Lambda^\Upsilon)^\dagger]_\omega$ represent $\mathcal{T}_\Lambda^\Upsilon$ and $(\mathcal{T}_\Lambda^\Upsilon)^\dagger$, respectively, evaluated at $\lambda_j^{(\omega)}$ ($j = 1, \dots, N$) and $\mu_k^{(\omega)}$ ($k = 1, \dots, N_c$).

We need to determine the nonzero singular value $\sigma_{\min}([(\mathcal{T}_\Lambda^\Upsilon)^\dagger]_\omega)$. For this purpose, deleting the last two zero-rows and zero-columns of $[(\mathcal{T}_\Lambda^\Upsilon)^\dagger]_\omega [(\mathcal{T}_\Lambda^\Upsilon)^\dagger]_\omega^*$ which correspond to two zero eigenvalues, the remaining algebraic manipulation is to pursue after the square root of the smallest nonzero eigenvalue of the complex Hermitian tridiagonal matrix

$$\begin{bmatrix} \zeta_2^{(\omega)} & -\rho_2^{(\omega)} & & & & & \\ -\bar{\rho}_2^{(\omega)} & \theta_2^{(\omega)} + \zeta_3^{(\omega)} & -\rho_3^{(\omega)} & & & & \\ & \ddots & \ddots & \ddots & & & \\ & & & -\bar{\rho}_{N_c-2}^{(\omega)} & \theta_{N_c-2}^{(\omega)} + \zeta_{N_c-1}^{(\omega)} & -\rho_{N_c-1}^{(\omega)} & \\ & & & & -\bar{\rho}_{N_c-1}^{(\omega)} & \theta_{N_c-1}^{(\omega)} + \zeta_{N_c}^{(\omega)} & \end{bmatrix} \quad (3.7)$$

with

$$\begin{aligned} \zeta_\epsilon^{(\omega)} &= \frac{1}{\left| \lambda_{(\epsilon-1)m}^{(\omega)} \cdots \lambda_{(\epsilon-2)m+1}^{(\omega)} \right|^2 \left| \lambda_{\epsilon m}^{(\omega)} \cdots \lambda_{(\epsilon-1)m+1}^{(\omega)} - \mu_\epsilon^{(\omega)} \right|^2}, \quad \epsilon = 2, \dots, N_c; \\ \rho_\varsigma^{(\omega)} &= \frac{\bar{\mu}_\varsigma^{(\omega)}}{\bar{\lambda}_{\varsigma m}^{(\omega)} \cdots \bar{\lambda}_{(\varsigma-1)m+1}^{(\omega)} \lambda_{(\varsigma-1)m}^{(\omega)} \cdots \lambda_{(\varsigma-2)m+1}^{(\omega)} \left| \lambda_{\varsigma m}^{(\omega)} \cdots \lambda_{(\varsigma-1)m+1}^{(\omega)} - \mu_\varsigma^{(\omega)} \right|^2}, \\ \theta_\varsigma^{(\omega)} &= \frac{|\mu_\varsigma^{(\omega)}|^2}{\left| \lambda_{\varsigma m}^{(\omega)} \cdots \lambda_{(\varsigma-1)m+1}^{(\omega)} \right|^2 \left| \lambda_{\varsigma m}^{(\omega)} \cdots \lambda_{(\varsigma-1)m+1}^{(\omega)} - \mu_\varsigma^{(\omega)} \right|^2}, \quad \varsigma = 2, \dots, N_c - 1. \end{aligned}$$

It is assumed throughout that the temporal eigenvalue approximation property (TEAP) is valid for each eigenmode ω with positive constants $\{\delta_\varsigma^{(\omega)}\}_{\varsigma=2}^{N_c-1}$:

$$\left| \lambda_{\varsigma m}^{(\omega)} \cdots \lambda_{(\varsigma-1)m+1}^{(\omega)} - \mu_\varsigma^{(\omega)} \right|^2 \leq \delta_\varsigma^{(\omega)} \left(\frac{1}{\left| \lambda_{(\varsigma-1)m}^{(\omega)} \cdots \lambda_{(\varsigma-2)m+1}^{(\omega)} \right|^2} - \frac{|\mu_\varsigma^{(\omega)}|}{\left| \lambda_{\varsigma m}^{(\omega)} \cdots \lambda_{(\varsigma-2)m+1}^{(\omega)} \right|} \right), \quad \varsigma = 2, \dots, N_c - 1. \quad (3.8)$$

Applying the Gershgorin circle theorem, it can be deduced that

$$\|\mathcal{T}_\Psi^\Phi\|_{(\tilde{\mathcal{X}}_s \tilde{\mathcal{X}}_s^*)^{-1}}^2 \leq \max_\omega \max \left\{ \delta_2^{(\omega)}, \max_{\varsigma=2, \dots, N_c-1} \frac{\delta_{\varsigma+1}^{(\omega)} \delta_\varsigma^{(\omega)} \left| \lambda_{\varsigma m}^{(\omega)} \cdots \lambda_{(\varsigma-1)m+1}^{(\omega)} \right|}{\delta_\varsigma^{(\omega)} \left| \lambda_{\varsigma m}^{(\omega)} \cdots \lambda_{(\varsigma-1)m+1}^{(\omega)} \right| - \delta_{\varsigma+1}^{(\omega)} |\mu_\varsigma^{(\omega)}| \left| \lambda_{(\varsigma-1)m}^{(\omega)} \cdots \lambda_{(\varsigma-2)m+1}^{(\omega)} \right|} \right\} \quad (3.9)$$

by making the crucial observations that

$$\frac{1}{\left| \lambda_{\varsigma m}^{(\omega)} \cdots \lambda_{(\varsigma-1)m+1}^{(\omega)} \right|^2 \left| \lambda_{(\varsigma+1)m}^{(\omega)} \cdots \lambda_{\varsigma m+1}^{(\omega)} - \mu_{\varsigma+1}^{(\omega)} \right|^2} - \frac{|\mu_{\varsigma+1}^{(\omega)}|}{\left| \lambda_{(\varsigma+1)m}^{(\omega)} \cdots \lambda_{(\varsigma-1)m+1}^{(\omega)} \right| \left| \lambda_{(\varsigma+1)m}^{(\omega)} \cdots \lambda_{\varsigma m+1}^{(\omega)} - \mu_{\varsigma+1}^{(\omega)} \right|^2} \geq \frac{1}{\delta_\varsigma^{(\omega)}}$$

and

$$\frac{1}{\left| \lambda_{\varsigma m}^{(\omega)} \cdots \lambda_{(\varsigma-1)m+1}^{(\omega)} - \mu_\varsigma^{(\omega)} \right|^2} \left(\frac{|\mu_\varsigma^{(\omega)}|^2}{\left| \lambda_{\varsigma m}^{(\omega)} \cdots \lambda_{(\varsigma-1)m+1}^{(\omega)} \right|^2} - \frac{|\mu_\varsigma^{(\omega)}|}{\left| \lambda_{\varsigma m}^{(\omega)} \cdots \lambda_{(\varsigma-2)m+1}^{(\omega)} \right|} \right) \geq -\frac{|\mu_\varsigma^{(\omega)}|}{\delta_\varsigma^{(\omega)}} \times \frac{\left| \lambda_{(\varsigma-1)m}^{(\omega)} \cdots \lambda_{(\varsigma-2)m+1}^{(\omega)} \right|}{\left| \lambda_{\varsigma m}^{(\omega)} \cdots \lambda_{(\varsigma-1)m+1}^{(\omega)} \right|}.$$

These four stages are summarized in the following theorem.

Theorem 1. Assume that Ψ_j and Φ_k are both strongly stable and simultaneously diagonalizable by X_s with eigenvalues $\{\lambda_j^{(\omega)}\}_{\omega=1}^n$ and $\{\mu_k^{(\omega)}\}_{\omega=1}^n$, respectively. Let $\sigma_{\min}^{(\omega)}$ be the smallest nonzero eigenvalue of (3.7). Then,

$$\|\mathcal{T}_\Psi^\Phi\|_{(\tilde{X}_s \tilde{X}_s^*)^{-1}} = \frac{1}{\min_{\omega} \sqrt{\sigma_{\min}^{(\omega)}}}. \quad (3.10)$$

If the TEAP condition (3.8) holds for all $\varsigma = 2, \dots, N_c - 1$ and $\omega = 1, \dots, n$, then (3.9) provides an actual upper bound. Furthermore,

$$\delta_2^{(\omega)} < 1 \text{ and } \frac{\delta_{\varsigma+1}^{(\omega)} \delta_{\varsigma}^{(\omega)} \left| \lambda_{\varsigma m}^{(\omega)} \cdots \lambda_{(\varsigma-1)m+1}^{(\omega)} \right|}{\delta_{\varsigma}^{(\omega)} \left| \lambda_{\varsigma m}^{(\omega)} \cdots \lambda_{(\varsigma-1)m+1}^{(\omega)} \right| - \delta_{\varsigma+1}^{(\omega)} \left| \mu_{\varsigma}^{(\omega)} \right| \left| \lambda_{(\varsigma-1)m}^{(\omega)} \cdots \lambda_{(\varsigma-2)m+1}^{(\omega)} \right|} < 1$$

are the sufficient conditions to ensure the convergence of the two-level version of Algorithm 1.

Remark 2. Notice that, for the particular case of the equidistant fine temporal mesh, (3.7) can be written as

$$\frac{1}{\left| (\lambda^{(\omega)})^m \right|^2 \left| (\lambda^{(\omega)})^m - \mu^{(\omega)} \right|^2} \mathcal{D}_\omega, \text{ where } \mathcal{D}_\omega = \begin{bmatrix} 1 & -\bar{\mu}^{(\omega)} & & & & \\ -\mu^{(\omega)} & 1 + |\mu^{(\omega)}|^2 & -\bar{\mu}^{(\omega)} & & & \\ & \ddots & \ddots & \ddots & & \\ & & & -\mu^{(\omega)} & 1 + |\mu^{(\omega)}|^2 & -\bar{\mu}^{(\omega)} \\ & & & & -\mu^{(\omega)} & 1 + |\mu^{(\omega)}|^2 \end{bmatrix}.$$

Following from the general result [68, equality (7)] and the necessary condition [68, equality (6)], it is not difficult to see that the smallest eigenvalue of \mathcal{D}_ω , denoted by $\lambda_{\min}(\mathcal{D}_\omega)$, is bounded by

$$(1 - |\mu^{(\omega)}|)^2 + \frac{\pi^2 |\mu^{(\omega)}|}{6(N_c - 1)^2} \leq \lambda_{\min}(\mathcal{D}_\omega) \leq (1 + |\mu^{(\omega)}|)^2 + \frac{\pi^2 |\mu^{(\omega)}|}{(N_c - 1)^2},$$

which can be derived from an argument analogous to that for [62, Lemma 36], where perturbations $\tilde{\alpha} = 0$ and $\tilde{\beta} = |\mu^{(\omega)}|^2$ are replaced by $\tilde{\alpha} = |\mu^{(\omega)}|^2$ and $\tilde{\beta} = 0$. Indeed, in this case, the upper bound (3.10) would be reduced to the tight bounds stated in [62, Theorem 30, inequality (63)]. Furthermore, it is apparent that Theorem 1 can be regarded as a generalization of [62, Theorem 35] to the FCF-relaxation case, which has been proven a key component used to build a scalable multilevel solver [54].

Remark 3. The $(\tilde{X}_s \tilde{X}_s^*)^{-1}$ -norm will be reduced to the discrete l^2 -norm only when the matrix X_s is unitary, that is, Ψ_j and Φ_k are both normal.

Remark 4. The upper bound (3.9) is usually not tight. Fortunately, the exact convergence upper bound (3.10) can be evaluated via hunting for the smallest eigenvalue of (3.7). Multitudinous research efforts on open-source packages have been made to deal with this issue, e.g., LAPACK, EISPACK, FEAST and PRIMME.

Remark 5. In the existing two-level convergence theory [60, 63], fine and coarse time-grid propagators are assumed to be unitarily diagonalizable (or, equivalently, normal matrices). However, this assumption is extremely strong and it probably isn't always true, even for [60, Example 4.1.2], where the linear operator G usually cannot be unitarily diagonalizable.

3.3. Specific application

For convenience of analysis we rewrite the time-marching loop (2.4) as, ignoring the auxiliary vectors $\{\mathcal{V}_j\}_{j=0}^N$:

$$(M_s + \tau_{k+1} Q_s) \mathcal{U}_{k+1} = M_s \mathcal{U}_k + \tau_{k+1} \mathcal{F}_{k+1}, \quad k = 0, \dots, N-1, \quad (3.11)$$

where the Schur complement

$$Q_s = (m_{11}^z A_s + a_{11}^z M_s) - (\tilde{m}_z \otimes A_s + \tilde{a}_z \otimes M_s)(\tilde{M}_z \otimes A_s + \tilde{A}_z \otimes M_s)^{-1}(\tilde{m}_z^T \otimes A_s + \tilde{a}_z^T \otimes M_s)$$

with vectors $\tilde{m}_z = (m_{12}^z, \dots, m_{1n}^z)$ and $\tilde{a}_z = (a_{12}^z, \dots, a_{1n}^z)$, as well as submatrices $\tilde{M}_z = (m_{ij}^z)_{i,j=2}^{M-1}$ and $\tilde{A}_z = (a_{ij}^z)_{i,j=2}^{M-1}$. The invertibility of $\tilde{M}_z \otimes A_s + \tilde{A}_z \otimes M_s$ is assured due to its positive definiteness, see [69, Proposition 2.1].

Regarding (3.11), the vector $\mathcal{G}_j = \tau_j(M_s + \tau_j Q_s)^{-1} \mathcal{F}_j$, the fine time-grid time-stepping scheme

$$\Psi_j = (M_s + \tau_j Q_s)^{-1} M_s, \quad j = 1, \dots, N \quad (3.12)$$

and the coarse-grid time-stepping scheme is given by

$$\Phi_k = (M_s + \tilde{\tau}_k Q_s)^{-1} M_s, \quad k = 1, \dots, N_c. \quad (3.13)$$

It should be emphasized that the aforementioned matrix inversion corresponds to a spatial solve, however, not by an appropriate solver for (3.11) but by the multigrid method with line smoother for (2.4).

Theorem 2. *Time-grid propagators (3.12) and (3.13) are both strongly stable.*

Proof. Viewed from the specific expressions (3.12) and (3.13), it is clear that Ψ_j ($j = 1, \dots, N$) and Φ_k ($k = 1, \dots, N_c$) can be simultaneously diagonalized by an appropriate matrix X_s which makes $M_s^{1/2} X_s$ unitary. The reason is that

$$\Psi_j = M_s^{-1/2} (I + \tau_j M_s^{-1/2} Q_s M_s^{-1/2})^{-1} M_s^{1/2} \Rightarrow (I + \tau_j M_s^{-1/2} Q_s M_s^{-1/2})^{-1} = M_s^{1/2} \Psi_j M_s^{-1/2},$$

which can be of course diagonalizable by the orthogonal matrix $M_s^{1/2} X_s$ because it is symmetric (real) to ensure its normality. It is important to notice that since matrices $(I + \tau_j M_s^{-1/2} Q_s M_s^{-1/2})^{-1}$ and $(I + \tilde{\tau}_k M_s^{-1/2} Q_s M_s^{-1/2})^{-1}$ are both SPD and respectively similar to Ψ_j and Φ_k , the ω -th eigenvalues of Ψ_j and Φ_k is calculated by

$$\lambda_j^{(\omega)} = \frac{1}{1 + \tau_j \sigma_\omega} \quad \text{and} \quad \mu_k^{(\omega)} = \frac{1}{1 + \tilde{\tau}_k \sigma_\omega}, \quad \omega = 1, \dots, n, \quad (3.14)$$

where σ_ω is the ω -th eigenvalue of the matrix $M_s^{-1/2} Q_s M_s^{-1/2}$. It is obvious that, for any eigenmode ω , eigenvalues $\lambda_j^{(\omega)}$ ($j = 1, \dots, N$) and $\mu_k^{(\omega)}$ ($k = 1, \dots, N_c$) are all real, positive and smaller than one due to the SPD property of $M_s^{-1/2} Q_s M_s^{-1/2}$ which makes $\sigma_\omega > 0$ for $\omega = 1, \dots, n$. This completes the proof. \blacksquare

Theorem 2 indicates that the two key assumptions in Stage S1 are satisfied, then, plugging (3.14), (3.7) becomes

$$\begin{bmatrix} \zeta_2^{(\omega)} & -\rho_2^{(\omega)} & & & & \\ -\rho_2^{(\omega)} & \theta_2^{(\omega)} + \zeta_3^{(\omega)} & -\rho_3^{(\omega)} & & & \\ & \ddots & \ddots & \ddots & & \\ & & & -\rho_{N_c-2}^{(\omega)} & \theta_{N_c-2}^{(\omega)} + \zeta_{N_c-1}^{(\omega)} & -\rho_{N_c-1}^{(\omega)} \\ & & & & -\rho_{N_c-1}^{(\omega)} & \theta_{N_c-1}^{(\omega)} + \zeta_{N_c}^{(\omega)} \end{bmatrix} \quad \begin{aligned} \zeta_\epsilon^{(\omega)} &= [\pi_{\epsilon-1}^{(\omega)} \pi_\epsilon^{(\omega)} (1 + \tilde{\tau}_\epsilon \sigma_\omega) \tilde{\pi}_\epsilon^{(\omega)}]^2, \\ \text{with } \rho_\zeta^{(\omega)} &= \pi_{\zeta-1}^{(\omega)} (\pi_\zeta^{(\omega)})^3 (1 + \tilde{\tau}_\zeta \sigma_\omega) (\tilde{\pi}_\zeta^{(\omega)})^2, \\ \theta_\zeta^{(\omega)} &= (\pi_\zeta^{(\omega)})^4 (\tilde{\pi}_\zeta^{(\omega)})^2, \end{aligned}$$

and the upper bound (3.9) becomes

$$\|\mathcal{T}_\Psi^\Phi\|_{(\tilde{\chi}, \tilde{\chi}_s^*)}^2 \leq \max_\omega \max \left\{ \delta_2^{(\omega)}, \max_{\zeta=2, \dots, N_c-1} \frac{\delta_{\zeta+1}^{(\omega)} \delta_\zeta^{(\omega)} (1 + \tilde{\tau}_\zeta \sigma_\omega) \pi_{\zeta-1}^{(\omega)}}{\delta_\zeta^{(\omega)} (1 + \tilde{\tau}_\zeta \sigma_\omega) \pi_{\zeta-1}^{(\omega)} - \delta_{\zeta+1}^{(\omega)} \pi_\zeta^{(\omega)}} \right\},$$

where

$$\pi_\zeta^{(\omega)} = \prod_{j=(\zeta-1)m+1}^{\zeta m} (1 + \tau_j \sigma_\omega), \quad \tilde{\pi}_\zeta^{(\omega)} = \frac{1}{1 + \tilde{\tau}_\zeta \sigma_\omega - \pi_\zeta^{(\omega)}}.$$

4. Numerical experimentations

Numerical results are reported to illustrate the convergence rate and the error-norms decay property of the fully discrete FE scheme (2.3), profile how robust should the multigrid with line smoother proposed in [27] be in regards to the fractional order α and the spatial mesh size, and evaluate how sharp is our derived convergence upper bound listed in Theorem 1, for solving problem (1.1) posed on a unit square and an L-shaped domains. All our numerical computations are carried out on a 64-bit Fedora 14 platform, in double precision arithmetic on Intel Xeon (W5590) with 24.0 gigabytes random access memory, 3.33 gigahertz and an -O2 compiler optimization option.

4.1. Order of convergence test

Example 1. Consider problem (1.1) with the reference solution $u = e^{-t} \sin(\pi x) \sin(\pi y)$ and $\Omega = (0, 1)^2$.

We partition the solution domain Ω into a uniform triangular mesh with size h_Ω , and construct a graded mesh in the extended direction using the formula (2.2) with the length $\mathcal{Z} = 1$. The finite element space and respective matrices were introduced in Section 2. The chosen time step sizes $\tau = 10^{-4}$ and $\tau = 5 \times 10^{-5}$. The tolerance for stopping of the multigrid V(1,1)-cycle algorithm (using the zero initial guess and one presmoothing and postsmoothing sweep performed by the vertical line smoother in red-black ordering) in solving linear systems is that the discrete l^2 -norm of the residual is reduced by a factor of 10^8 relative to that of the initial residual.

Table 1 shows the number of degrees of freedom (DoF), the error-norms

$$\|e\|_N^\tau := \|u_N^\tau - u(x, y, N\tau)\|_{H^1(\mathcal{Z}^\beta)}, \quad \|e\|_{\max}^\tau := \max_{j=1, \dots, N} \|u_j^\tau - u(x, y, j\tau)\|_{H^1(\mathcal{Z}^\beta)},$$

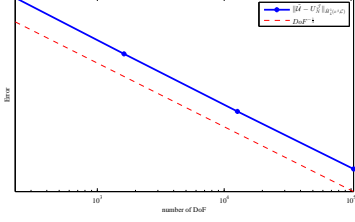
the respective rate computed by the error of the coarser grid divided by that of the current grid, and the average number of iterations for multigrid required to achieve convergence for $\alpha = 0.4, 1.0$ and 1.4 . In these cases, the results are all in agreement with theory, and the multigrid V(1,1)-cycle is almost uniform with respect to the fractional order α and the number of DoF (or, equivalently, the spatial mesh size h_Ω). In particular, looking at Fig. 2 we can observe that the computational error-norm decay rate in $\|\tilde{\mathcal{U}} - U_N^\tau\|_{\hat{H}_L^1(\mathcal{Z}^\beta, C)}$ is about $\text{DoF}^{-1/3}$.

Table 1: Error results, convergence rates and average number of iterations for three different α and two different τ .

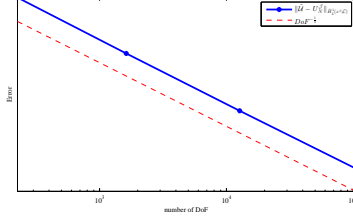
α	h_Ω	DoF	$\ e\ _{100}^{1e-4}$	rate	$\ e\ _{\max}^{1e-4}$	rate	aIter	$\ e\ _{200}^{5e-5}$	rate	$\ e\ _{\max}^{5e-5}$	rate	aIter
0.4	1/4	225	8.37e-1		8.42e-1		11	8.39e-1		8.42e-1		11
	1/8	1620	4.28e-1	1.96	4.43e-1	1.90	12	4.29e-1	1.96	4.30e-1	1.96	12
	1/16	12716	2.16e-1	1.98	2.17e-1	2.04	12	2.16e-1	1.99	2.17e-1	1.98	11
	1/32	104544	1.09e-1	1.98	1.10e-1	1.97	12	1.09e-1	1.98	1.10e-1	1.97	12
	1/64	887250	5.58e-2	1.95	5.87e-2	1.87	12	5.58e-2	1.95	5.87e-2	1.87	12
1.0	1/4	225	8.39e-1		8.42e-1		11	8.37e-1		8.42e-1		11
	1/8	1620	4.30e-1	1.95	4.30e-1	1.96	12	4.28e-1	1.96	4.30e-1	1.96	12
	1/16	12716	2.16e-1	1.99	2.17e-1	1.98	13	2.15e-1	1.99	2.17e-1	1.98	12
	1/32	104544	1.09e-1	1.98	1.10e-1	1.97	13	1.08e-1	1.99	1.10e-1	1.97	13
	1/64	887250	5.40e-2	2.02	5.86e-2	1.88	13	5.40e-2	2.00	5.86e-2	1.88	13
1.4	1/4	225	8.35e-1		8.42e-1		11	8.36e-1		8.42e-1		11
	1/8	1620	4.28e-1	1.95	4.30e-1	1.96	12	4.28e-1	1.95	4.30e-1	1.96	12
	1/16	12716	2.16e-1	1.98	2.17e-1	1.98	13	2.16e-1	1.98	2.17e-1	1.98	13
	1/32	104544	1.09e-1	1.98	1.10e-1	1.97	13	1.09e-1	1.98	1.10e-1	1.97	13
	1/64	887250	5.60e-2	1.95	5.85e-2	1.88	14	5.60e-2	1.95	5.86e-2	1.88	13

Example 2. Consider problem (1.1) with the reference solution $u = e^{-t} \sin(\pi x) \sin(\pi y)$ and $\Omega = (-1, 1)^2 \setminus (0, 1)^2$.

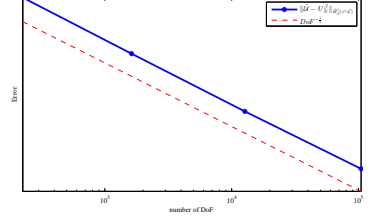
Fig. 3 illustrates the computational error-norm decays, numerical solutions and absolute errors of the reference solution and numerical solution with $\alpha = 0.4, 1.0$ and 1.4 . In three cases, we again obtain that the computational error-norm decay rate $\approx \text{DoF}^{-1/3}$ and the fully discrete FE approximation is in much better agreement with the reference solution.



(a) $\alpha = 0.4$

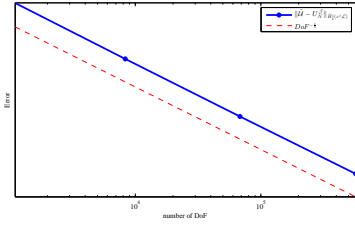


(b) $\alpha = 1.0$

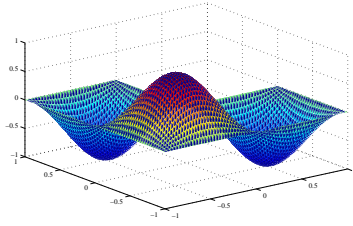


(c) $\alpha = 1.4$

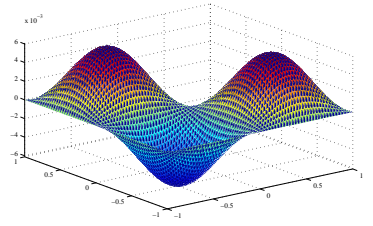
Figure 2: Computational error-norm decays as functions of DoF at $T = 0.01$ of Example 1, $\tau = 5 \times 10^{-5}$.



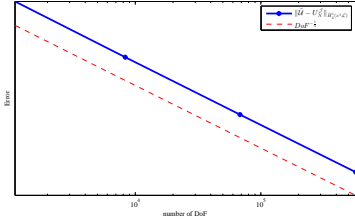
(a) $\alpha = 0.4$: error-norm decay



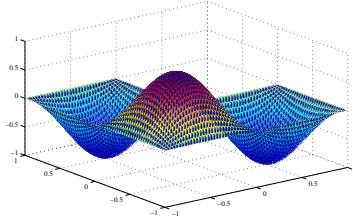
(b) $\alpha = 0.4$: numerical solution



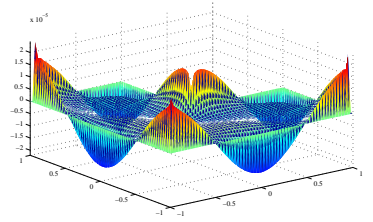
(c) $\alpha = 0.4$: absolute errors



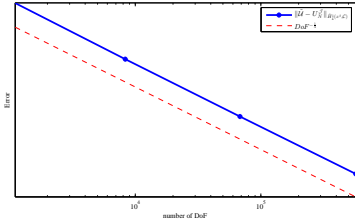
(d) $\alpha = 1.0$: error-norm decay



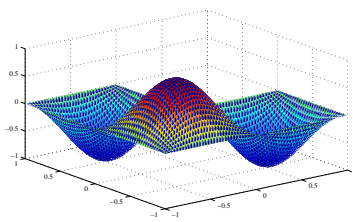
(e) $\alpha = 1.0$: numerical solution



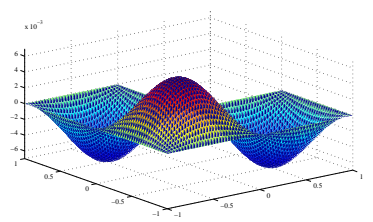
(f) $\alpha = 1.0$: absolute errors



(g) $\alpha = 1.4$: error-norm decay



(h) $\alpha = 1.4$: numerical solution



(i) $\alpha = 1.4$: absolute errors

Figure 3: Computational error-norm decays, numerical solutions and absolute errors at $T = 0.01$ of Example 2, $h_\Omega = 1/32$, $\tau = 5 \times 10^{-5}$.

4.2. Sharpness test in the convergence upper bound

In this subsection, the MGRIT V(1,0)-cycle algorithm using FCF-relaxation depicted in subsection 3.1 together with the MGRIT V(1,0)-cycle algorithm with F-relaxation (an equivalent version of parareal) are exploited for problem (1.1), where we take the maximum number of time levels $L = 2$. We principally investigate the sharpness of [62, Theorem 35] and Theorem 1 in the present paper, each of them is appended with \sqrt{m} from Stage S2 in subsection 3.2, by a comparison with the largest observed convergence factor in terms of $\max_i \{\|r_{i+1}\|/\|r_i\|\}$, where r_i is the residual vector obtained at the i -th iteration. To this end, we consider the spatial domains $\Omega = (0, 1)^2$ and $\Omega = (-1, 1)^2 \setminus (0, 1)^2$, and the final time $T = 1$. The spatial discretization takes advantage of the uniform triangulation with the grid spacing $h_\Omega = 1/8$. The uniform and graded temporal partitions are involved. The graded temporal mesh is defined by points $t_k = (k/N)^\varpi$ [70] for the parameter $\varpi = 5/2$. The considered number of time periods $N \in \{256, 1024, 4096\}$ and the coarsening factor $m \in \{2, 4, 8, 16\}$. The space-time approximation is achieved until the discrete l^2 space-time residual norm is smaller than the absolute halting tolerance 10^{-8} , along with 100 as the maximum number of MGRIT iterations.

All test cases are implemented in C, using the open-source packages XBraid and LAPACK. Furthermore, random initial guesses are selected for the entire temporal grid hierarchy beyond the initial condition in (1.1) is used at $t = 0$ on the finest grid.

Results for uniform temporal partition are shown in Fig. 4, demonstrating that, in this case, all observed convergence factors are smaller than and quite close to their theoretical upper bounds. It is indicated that single-iteration upper bounds proposed in [62, Theorem 30] (two particular cases of [62, Theorem 35] and Theorem 1) are tight. Another observation is that results for F-relaxation are slightly larger than those based on FCF-relaxation, even though the former corresponds to an optimal two-level algorithm. Furthermore, it must be emphasized that they decrease as the number of time periods N increases while tend to become larger as the coarsening factor m increases.

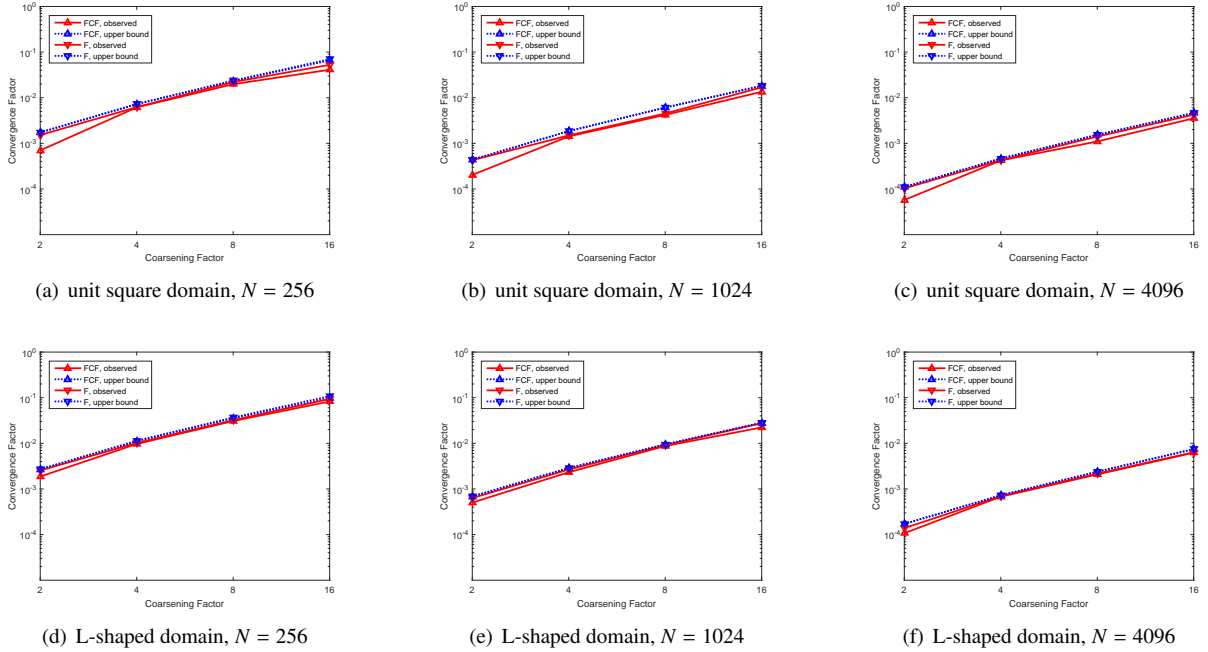


Figure 4: Uniform temporal partition: comparison on the convergence behavior of the two-level MGRIT V(1,0)-cycle with F- and FCF-relaxation.

Fig. 5 reports the sharpness results in the graded temporal mesh, where we notice again that the upper bounds on the two-level MGRIT V(1,0)-cycle convergence described in [62, Theorem 35] and Theorem 1 are tight (see Fig. 5(a), 5(b), 5(d) and 5(e)), whereas the upper bound provided in [63, Theorem 2, inequality (3.4)] is not a good indicator, sometimes even greater than one (see Fig. 5(c) and 5(f)). Similar to the uniform case, the predicted and the largest

observed convergence factors grow with the coarsening factor but decrease with the number of time periods. Again, FCF-relaxation yields a slightly quicker convergence.

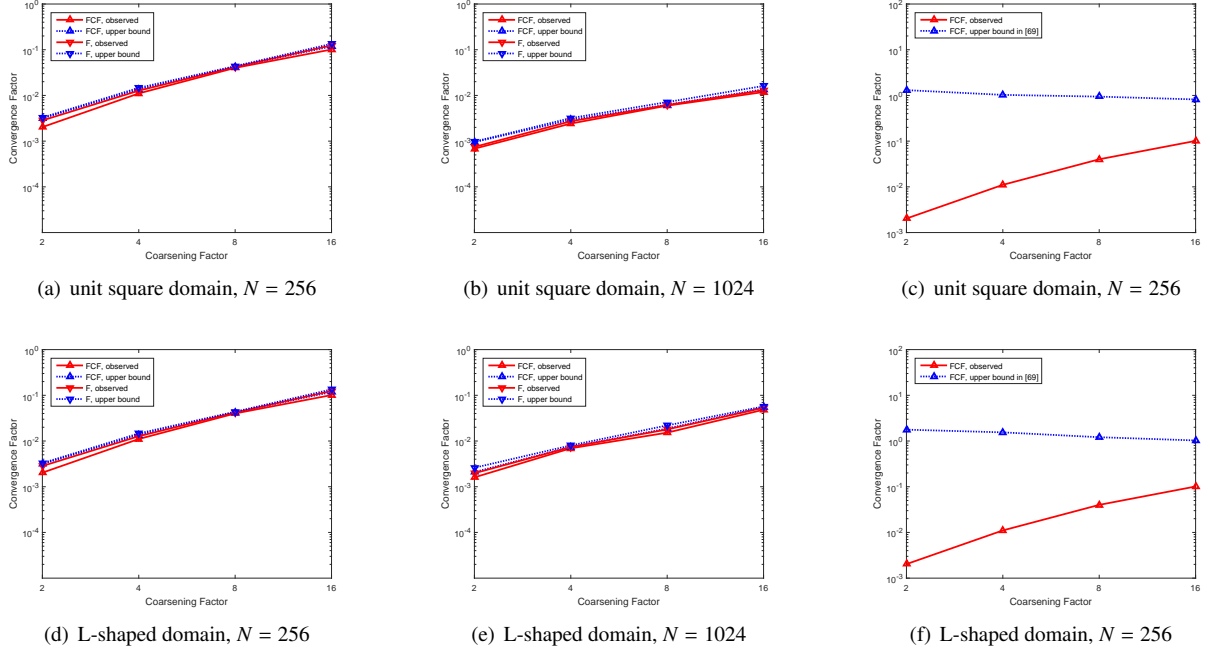


Figure 5: Graded temporal mesh: comparison on the convergence behavior of the two-level MGRIT V(1,0)-cycle with F- and FCF-relaxation.

5. Conclusions

In this work, we provided a generalized two-level convergence theory of the MGRIT V(1,0)-cycle algorithm with FCF-relaxation and time-dependent time-grid propagators, and sufficient conditions for the convergence of the two-level variant in light of a new TEAP condition. The generalization is reflected by removing the unitary diagonalization assumption, inspired by Southworth [62]. Numerical experiments with respect to two-dimensional unsteady fractional Laplacian problems show consistency with the theoretical results and sharpness with our analysis. Extensions of this method to time fractional problems [71–74] or to support problems with adaptive time stepping [75] are the subject of current research.

Acknowledgement

This work is financially supported by the National Natural Science Foundation of China (11571293, 11601462, 11701197, 41874086), Project of Scientific Research Fund of Hunan Provincial Science and Technology Department (2018WK4006), Excellent Youth Foundation of Hunan Province of China (2018JJ1042) and Hunan Provincial Natural Science Foundation of China (2018JJ3494). We are indebted to Prof. L. Chen from University of California at Irvine for providing the software package *iFEM* [76].

References

References

- [1] C. Pozrikidis, The fractional Laplacian, Chapman and Hall/CRC, 2016.
- [2] J. R. Wang, M. Fečkan and Y. Zhou, A survey on impulsive fractional differential equations, *Fract. Calc. Appl. Anal.* 19 (2016), pp. 806-831.

- [3] J. T. Machado, V. Kiryakova and F. Mainardi, Recent history of fractional calculus, *Commun. Nonlinear Sci.* 16 (2011), pp. 1140-1153.
- [4] S. Chen, F. Liu and K. Burrage, Numerical simulation of a new two-dimensional variable-order fractional percolation equation in non-homogeneous porous media, *Comput. Math. Appl.* 68 (2014), pp. 2133-2141.
- [5] A. I. Saichev and G. M. Zaslavsky, Fractional kinetic equations: solutions and applications, *Chaos* 7 (1997), pp. 753-764.
- [6] N. Laskin, Fractional quantum mechanics and Lévy path integrals, *Phys. Lett. A* 268 (2000), pp. 298-305.
- [7] R. Cont and E. Voltchkova, A finite difference scheme for option pricing in jump diffusion and exponential Lévy models, *SIAM J. Numer. Anal.* 43 (2005), pp. 1596-1626.
- [8] S. Dipierro, G. Palatucci and E. Valdinoci, Dislocation dynamics in crystals: a macroscopic theory in a fractional Laplace setting, *Commun. Math. Phys.* 333 (2015), pp. 1061-1105.
- [9] A. de Pablo, F. Quirós, A. Rodríguez and J. L. Vázquez, A fractional porous medium equation, *Adv. Math.* 226 (2011), pp. 1378-1409.
- [10] T. Gao, J. Duan, X. Li and R. Song, Mean exit time and escape probability for dynamical systems driven by Lévy noises, *SIAM J. Sci. Comput.* 36 (2014), pp. A887-A906.
- [11] A. Lischke et al., What is the fractional Laplacian? arXiv: 1801.09767.
- [12] Y. H. Huang and A. Oberman, Numerical methods for the fractional Laplacian: a finite difference-quadrature approach, *SIAM J. Numer. Anal.* 52 (2014), pp. 3056-3084.
- [13] D. L. Wang, A. G. Xiao and W. Yang, A linearly implicit conservative difference scheme for the space fractional coupled nonlinear Schrödinger equations, *J. Comput. Phys.* 272 (2014), pp. 644-655.
- [14] W. Yang, D. L. Wang and L. Yang, A stable numerical method for space fractional Landau-Lifshitz equations, *Appl. Math. Lett.* 61 (2016), pp. 149-155.
- [15] B. J. Szekeres and F. Izsák, Finite difference approximation of space-fractional diffusion problems: the matrix transformation method, *Comput. Math. Appl.* 73 (2017), pp. 261-269.
- [16] D. D. He and K. J. Pan, An unconditionally stable linearized CCD-ADI method for generalized nonlinear Schrödinger equations with variable coefficients in two and three dimensions, *Comput. Math. Appl.* 73 (2017), pp. 2360-2374.
- [17] H. Fu, W. E. Zhou, X. Qian and S. H. Song, Novel conformal structure-preserving algorithms for coupled damped nonlinear Schrödinger system, *Adv. Appl. Math. Mech.* 9 (2017), pp. 1383-1403.
- [18] J. J. Wang, A. G. Xiao and C. X. Wang, A conservative difference scheme for space fractional Klein-Gordon-Schrödinger equations with a high-degree Yukawa interaction, *East Asia. J. Appl. Math.* 8 (2018), pp. 715-745.
- [19] J. J. Wang and A. G. Xiao, An efficient conservative difference scheme for fractional Klein-Gordon-Schrödinger equations, *Appl. Math. Comput.* 320 (2018), pp. 691-709.
- [20] S. W. Duo, H. W. van Wyk and Y. Z. Zhang, A novel and accurate finite difference method for the fractional Laplacian and the fractional Poisson problem, *J. Comput. Phys.* 355 (2018), pp. 233-252.
- [21] M. Li, A high-order split-step finite difference method for the system of the space fractional CNLS, *Eur. Phys. J. Plus* 134 (2019), pp. 244.
- [22] O. Karakashian and C. Makridakis, A space-time finite element method for the nonlinear Schrödinger equation: the continuous Galerkin method, *SIAM J. Numer. Anal.* 36 (1999), pp. 1779-1807.
- [23] J. C. Jin and X. N. Wu, Analysis of finite element method for one-dimensional time-dependent Schrödinger equation on unbounded domain, *J. Comput. Appl. Math.* 220 (2008), pp. 240-256.
- [24] R. H. Nochetto, E. Otárola and A. J. Salgado, A PDE approach to fractional diffusion in general domains: a priori error analysis, *Found. Comput. Math.* 15 (2015), pp. 733-791.
- [25] P. Gatto and J. S. Hesthaven, Numerical approximation of the fractional Laplacian via hp-finite elements, with an application to image denoising, *J. Sci. Comput.* 65 (2015), pp. 249-270.
- [26] J. Y. Wang, Y. Q. Huang, Z. K. Tian and J. Zhou, Superconvergence analysis of finite element method for the time-dependent Schrödinger equation, *Comput. Math. Appl.* 71 (2016), pp. 1960-1972.
- [27] L. Chen, R. H. Nochetto, E. Otárola and A. J. Salgado, Multilevel methods for nonuniformly elliptic operators and fractional diffusion, *Math. Comput.* 85 (2016), pp. 2583-2607.
- [28] G. Acosta and J. P. Borthagaray, A fractional Laplace equation: regularity of solutions and finite element approximations, *SIAM J. Numer. Anal.* 55 (2017), pp. 472-495.
- [29] M. Ainsworth and C. Glusa, Hybrid finite element-spectral method for the fractional Laplacian: approximation theory and efficient solver, *SIAM J. Sci. Comput.* 40 (2018), pp. A2383-A2405.
- [30] Q. Yang, I. Turner, T. Moroney and F. Liu, A preconditioned Lanczos method for space-fractional reaction-diffusion equations on two-dimensional unstructured meshes, in: 4th International Conference on Computational Methods, 2012.
- [31] W. Gao, H. Li, Y. Liu and X. X. Wei, A Padé compact high-order finite volume scheme for nonlinear Schrödinger equations, *Appl. Numer. Math.* 85 (2014), pp. 115-127.
- [32] A. A. Aderogba, M. Chapwanya, J. Djoko Kamdem and J. M.-S. Lubuma, Coupling finite volume and nonstandard finite difference schemes for a singularly perturbed Schrödinger equation, *Int. J. Comput. Math.* 93 (2016), pp. 1833-1844.
- [33] Q. W. Xu and J. S. Hesthaven, Discontinuous Galerkin method for fractional convection-diffusion equations, *SIAM J. Numer. Anal.* 52 (2014), pp. 405-423.
- [34] W. Y. Lu, Y. Q. Huang and H. L. Liu, Mass preserving discontinuous Galerkin methods for Schrödinger equations, *J. Comput. Phys.* 282 (2015), pp. 210-226.
- [35] R. P. Zhang, X. J. Yu, M. J. Li and X. G. Li, A conservative local discontinuous Galerkin method for the solution of nonlinear Schrödinger equation in two dimensions, *Sci. China Math.* 60 (2017), pp. 2515-2530.
- [36] T. Aboelenen, A direct discontinuous Galerkin method for fractional convection-diffusion and Schrödinger-type equations, *Eur. Phys. J. Plus* 133 (2018), 316.
- [37] A. Bueno-Orovio, D. Kay and K. Burrage, Fourier spectral methods for fractional-in-space reaction-diffusion equations, *BIT Numer. Math.* 54 (2014), pp. 937-954.
- [38] S. W. Duo and Y. Z. Zhang, Mass-conservative Fourier spectral methods for solving the fractional nonlinear Schrödinger equation, *Comput.*

- Math. Appl. 71 (2016), pp. 2257-2271.
- [39] Z. P. Mao and J. Shen, Hermite spectral methods for fractional PDEs in unbounded domains, *SIAM J. Sci. Comput.* 39 (2017), pp. A1928-A1950.
 - [40] Z. F. Weng, S. Y. Zhai and X. L. Feng, A Fourier spectral method for fractional-in-space Cahn-Hilliard equation, *Appl. Math. Model.* 42 (2017), pp. 462-477.
 - [41] Y. Q. Huang, X. Y. Li and A. G. Xiao, Fourier pseudospectral method on generalized sparse grids for the space-fractional Schrödinger equation, *Comput. Math. Appl.* 75 (2018), pp. 4241-4255.
 - [42] H. Zhang, X. Y. Jiang, C. Wang and S. Z. Chen, Crank-Nicolson Fourier spectral methods for the space fractional nonlinear Schrödinger equation and its parameter estimation, *Int. J. Comput. Math.* 96 (2019), pp. 238-263.
 - [43] J. J. Wang and A. G. Xiao, Conservative Fourier spectral method and numerical investigation of space fractional Klein-Gordon-Schrödinger equations, *Appl. Math. Comput.* 350 (2019), pp. 348-365.
 - [44] W. Zeng, A. G. Xiao and X. Y. Li, Error estimate of Fourier pseudo-spectral method for multidimensional nonlinear complex fractional Ginzburg-Landau equations, *Appl. Math. Lett.* 93 (2019), pp. 40-45.
 - [45] K. L. Xu and E. Darve, Spectral method for the fractional Laplacian in 2D and 3D, arXiv: 1812.08325.
 - [46] T. Tang, L. Wang, H. F. Yuan and T. Zhou, Rational spectral methods for PDEs involving fractional Laplacian in unbounded domains, arXiv: 1905.02476.
 - [47] A. Capella, J. Dávila, L. Dupaigne and Y. Sire, Regularity of radial extremal solutions for some non-local semilinear equations, *Commun. Part. Diff. Eq.* 36 (2011), pp. 1353-1384.
 - [48] R. G. Durán and A. L. Lombardi, Error estimates on anisotropic Q_1 elements for functions in weighted Sobolev spaces, *Math. Comput.* 74 (2005), pp. 1679-1706.
 - [49] R. H. Nochetto, E. Otárola and A. J. Salgado, A PDE approach to space-time fractional parabolic problems, *SIAM J. Numer. Anal.* 54 (2016), pp. 848-873.
 - [50] J. Nievergelt, Parallel methods for integrating ordinary differential equations, *Comm. ACM* 7 (1964), pp. 731-733.
 - [51] W. Miranker and W. Liniger, Parallel methods for the numerical integration of ordinary differential equations, *Math. Comput.* 21 (1967), pp. 303-320.
 - [52] M. J. Gander, 50 years of time parallel time integration, *Contrib. Math. Comput. Sci.* 9 (2015), pp. 69-114.
 - [53] J. L. Lions, Y. Maday and G. Turinici, Résolution d'EDP par un schéma en temps pararéel, *C. R. Acad. Sci. Paris Série I Math.* 332 (2001), pp. 661-668.
 - [54] R. D. Falgout, S. Friedhoff, Tz. V. Kolev, S. P. Maclachlan and J. B. Schroder, Parallel time integration with multigrid, *SIAM J. Sci. Comput.* 36 (2014), pp. C635-C661.
 - [55] S. L. Wu and T. Zhou, Fast parareal iterations for fractional diffusion equations, *J. Comput. Phys.* 329 (2017), pp. 210-226.
 - [56] S. L. Wu, An efficient parareal algorithm for a class of time-dependent problems with fractional Laplacian, *Appl. Math. Comput.* 307 (2017), pp. 329-341.
 - [57] S. L. Wu and T. Zhou, Parareal algorithms with local time-integrators for time fractional differential equations, *J. Comput. Phys.* 358 (2018), pp. 135-149.
 - [58] M. J. Gander and S. Vandewalle, Analysis of the parareal time-parallel time-integration method, *SIAM J. Sci. Comput.* 29 (2007), pp. 556-578.
 - [59] XBraid: Parallel multigrid in time. <http://lnl.gov/casc/xbraid>.
 - [60] V. A. Dobrev, Tz. Kolev, N. A. Petersson and J. B. Schroder, Two-level convergence theory for multigrid reduction in time (MGRIT), *SIAM J. Sci. Comput.* 39 (2017), pp. S501-S527.
 - [61] A. Hesselthaler, B. S. Southworth, D. Nordsletten, O. Röhrle, R. D. Falgout and J. B. Schroder, Multilevel convergence analysis of multigrid-reduction-in-time, arXiv: 1812.11508.
 - [62] B. S. Southworth, Necessary conditions and tight two-level convergence bounds for parareal and multigrid reduction in time, *SIAM J. Matrix Anal. Appl.* 40 (2019), pp. 564-608.
 - [63] X. Q. Yue, S. Shu, X. W. Xu, W. P. Bu and K. J. Pan, Parallel-in-time multigrid for space-time finite element approximations of two-dimensional space-fractional diffusion equations, *Comput. Math. Appl.* (2019) <https://doi.org/10.1016/j.camwa.2019.05.017>.
 - [64] V. Gol'dshtein and A. Ukhlov, Weighted Sobolev spaces and embedding theorems, *Trans. Amer. Math. Soc.* 361 (2009), pp. 3829-3850.
 - [65] B. Muckenhoupt, Weighted norm inequalities for the Hardy maximal function, *Trans. Amer. Math. Soc.* 165 (1972), pp. 207-226.
 - [66] M. Ries and U. Trottenberg, MGR-ein blitzschneller elliptischer löser, Tech. Report Preprint 277 SFB 72, Universität Bonn, 1979.
 - [67] R. J. LeVeque, Finite difference methods for ordinary and partial differential equations: steady-state and time-dependent problems, Society for Industrial and Applied Mathematics, 2007.
 - [68] W. C. Yueh, Eigenvalues of several tridiagonal matrices, *Appl. Math. E-Notes* 5 (2005), pp. 66-74.
 - [69] J. Gallier, The Schur complement and symmetric positive semidefinite (and definite) matrices, Technical Report, Penn Engineering, 2019.
 - [70] W. P. Bu, S. Shu, X. Q. Yue, A. G. Xiao and W. Zeng, Space-time finite element method for the multi-term time-space fractional diffusion equation on a two-dimensional domain, *Comput. Math. Appl.* (2018) <http://dx.doi.org/10.1016/j.camwa.2018.11.033>.
 - [71] Y. Yang, Y. P. Chen, Y. Q. Huang and H. Y. Wei, Spectral collocation method for the time-fractional diffusion-wave equation and convergence analysis, *Comput. Math. Appl.* 73 (2017), pp. 1218-1232.
 - [72] W. P. Bu, A. G. Xiao and W. Zeng, Finite difference/finite element methods for distributed-order time fractional diffusion equations, *J. Sci. Comput.* 72 (2017), pp. 422-441.
 - [73] Y. Yang, Y. Q. Huang and Y. Zhou, Numerical simulation of time fractional Cable equations and convergence analysis, *Numer. Methods Partial Differ. Equ.* 34 (2018), pp. 1556-1576.
 - [74] Y. Zhou, L. Peng and Y. Q. Huang, Duhamel's formula for time-fractional Schrödinger equations, *Math. Meth. Appl. Sci.* 41 (2018), pp. 8345-8349.
 - [75] J. G. Huang, J. J. Lai and T. Tang, An adaptive time stepping method with efficient error control for second-order evolution problems, *Sci. China Math.* 56 (2013), pp. 2753-2771.

- [76] L. Chen, *iFEM*: an integrated finite element methods package in MATLAB, Technical Report, University of California at Irvine, 2009.